

AD-A089 110 DAVID W TAYLOR NAVAL SHIP RESEARCH AND DEVELOPMENT CE--ETC F/6 13/8
ANALYSIS OF RESIDUAL STRESSES RESULTING FROM COLD ROLLING OF NO--ETC(U)
AUG 80 M G VASSILAROS
UNCLASSIFIED DTNSRDC/SME-80/23 NL

DAVID W TAYLOR NAVAL SHIP RESEARCH AND DEVELOPMENT CE--ETC F/G 13/8
ANALYSIS OF RESIDUAL STRESSES RESULTING FROM COLD ROLLING OF NO--ETC(U)
AUG 80 M G VASSILAROS
DTNSRDC SME-80/23 NL

UNCLASSIFIED

NL

∫ ∂ ∫

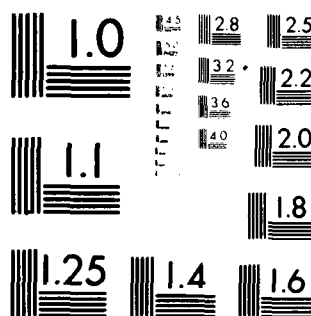
2. The following table shows the number of people who attended the concert in each age group.

END

DATE _____

10-80

DT10



MICROCOPY RESOLUTION TEST CHART
NATIONAL BUREAU OF STANDARDS-1963-A

DTNSRDC/SME-80/23

ANALYSIS OF RESIDUAL STRESSES RESULTING FROM COLD ROLLING OF NOTCHES
AND THEIR EFFECT ON FATIGUE BEHAVIOR

AD A089110

DDC FILE COPY

1st 1980

LEVEL

12 B.S.

DAVID W. TAYLOR NAVAL SHIP
RESEARCH AND DEVELOPMENT CENTER

Bethesda, Maryland 20884



ANALYSIS OF RESIDUAL STRESSES RESULTING FROM
COLD ROLLING OF NOTCHES AND THEIR EFFECT
ON FATIGUE BEHAVIOR

by
M. G. Vassilaros

DTIC
SELECTED
SEP 11 1980

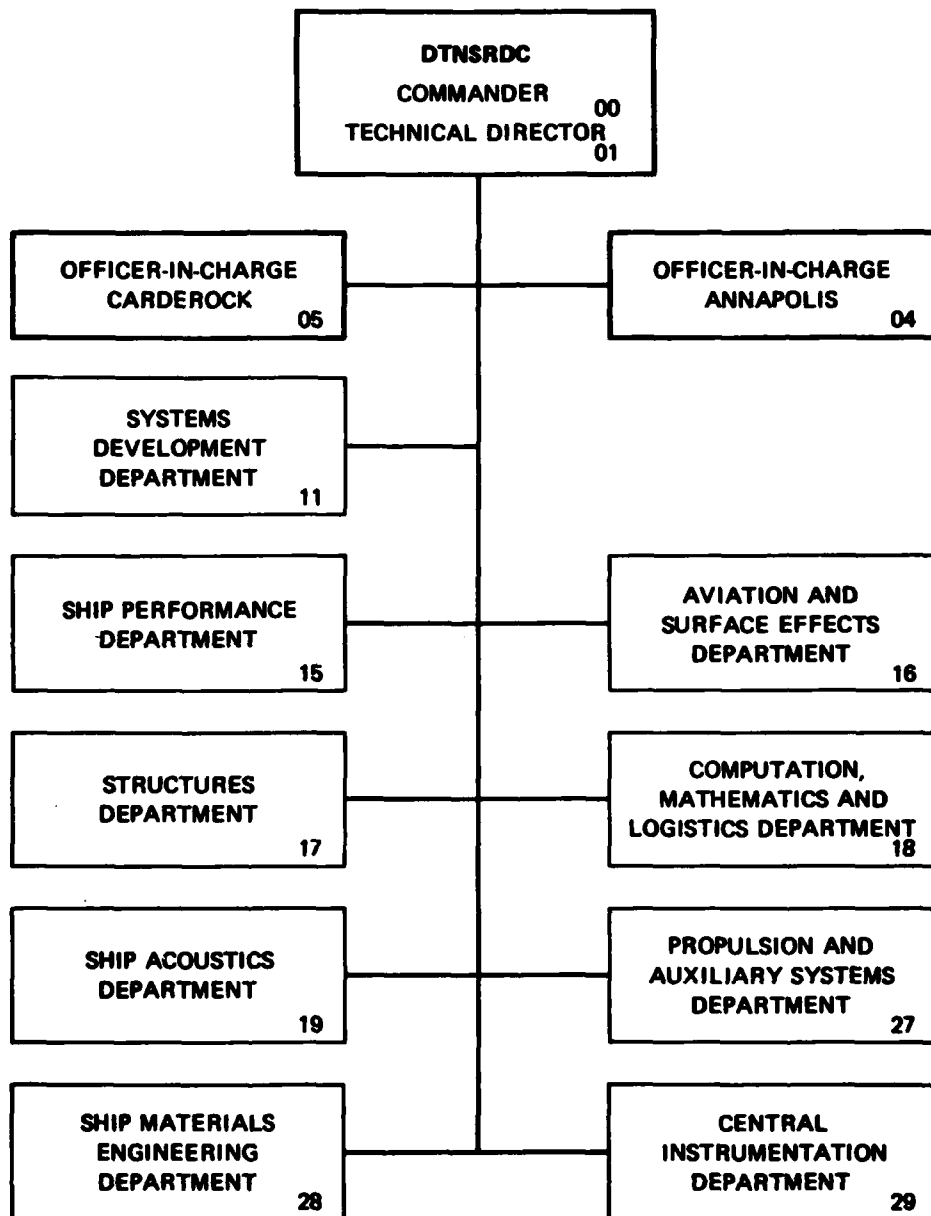
APPROVED FOR PUBLIC RELEASE; DISTRIBUTION UNLIMITED

SHIP MATERIALS ENGINEERING DEPARTMENT
RESEARCH AND DEVELOPMENT REPORT

DTNSRDC/SME-80/23

80 9 10 055

MAJOR DTNSRDC ORGANIZATIONAL COMPONENTS



(14) DINE /SME-1/

REPORT DOCUMENTATION PAGE		READ INSTRUCTIONS BEFORE COMPLETING FORM	
1. REPORT NUMBER	2. GOVT ACCESSION NO.	3. RECIPIENT'S CATALOG NUMBER	
	AD-A089 110		
4. TITLE (and Subtitle)		5. TYPE OF REPORT & PERIOD COVERED	
ANALYSIS OF RESIDUAL STRESSES RESULTING FROM COLD ROLLING OF NOTCHES AND THEIR EFFECT ON FATIGUE BEHAVIOR		Research & Development	
7. AUTHOR(s)		6. PERFORMING ORG. REPORT NUMBER	
M. G. Vassilaros			
9. PERFORMING ORGANIZATION NAME AND ADDRESS		8. CONTRACT OR GRANT NUMBER(s)	
David W. Taylor Naval Ship R&D Center Bethesda, MD 20084		D411	
11. CONTROLLING OFFICE NAME AND ADDRESS		10. PROGRAM ELEMENT, PROJECT, TASK AREA & WORK UNIT NUMBERS	
Naval Sea Systems Command (SEA 05R15) Washington, DC 20362		(See reverse side)	
14. MONITORING AGENCY NAME & ADDRESS (if different from Controlling Office)		12. REPORT DATE	
SLC 11		August 1980	
10, SL 011		13. NUMBER OF PAGES	
		38	
16. DISTRIBUTION STATEMENT (of this Report)		15. SECURITY CLASS. (of this report)	
		UNCLASSIFIED	
		15a. DECLASSIFICATION/DOWNGRADING SCHEDULE	
17. DISTRIBUTION STATEMENT (of the abstract entered in Block 20, if different from Report)			
18. SUPPLEMENTARY NOTES			
19. KEY WORDS (Continue on reverse side if necessary and identify by block number)			
Fatigue		Finite-Element Analysis	
Inconel		Notch Rolling	
Plasticity		Residual Stresses	
Slip-Line Fields			
20. ABSTRACT (Continue on reverse side if necessary and identify by block number)			
<p>The effects of cold forming on the fatigue behavior of threads were analyzed using slip-line field and finite-element analyses. Bolt threads were simulated using notched rotating cantilever-beam fatigue specimens of Inconel 718. The slip-line fields for wedge indentations, with some modifications, were used to analyze the deformation process of notch rolling. Stresses on the deepest slip lines were used in an elastic finite-element</p> <p>(Continued on reverse side)</p>			

UNCLASSIFIED

SECURITY CLASSIFICATION OF THIS PAGE (When Data Entered)

(Block 10)

Project 2803-160
Element 62761N
Work Unit 2814-181
Task Area 50379, SL001, Task 19979

(Block 20 continued)

→ analysis of the internal stresses existing outside the slip-line field during deformation. Negatives of the loads on the notch surface from the indenter were used in a second elastic finite-element analysis to determine the internal stresses resulting from unloading. These two stress analyses, with a correction for yielding, were employed to map the residual stress distribution around the rolled notch. The predicted residual stress distribution showed an intense compressive region below the notch root. However, a short distance away from and to the side of the notch, there began a region of residual tensile stresses.

This stress distribution was then used to rationalize the fatigue crack propagation behavior of Inconel 718 rotating cantilever-beam fatigue specimens with rolled and machined notches. When specimens with machined notches were fatigue tested, the crack propagation direction was perpendicular to the axis of rotation and in the direction of the maximum alternating stress gradient. In the presence of a rolled notch the crack propagation path was altered to a direction 50° from the perpendicular to the axis of rotation. This change was attributed to the residual stress distribution around the notch as indicated by the stress analysis. This change in the direction of crack propagation also reduced the magnitude of the alternating stresses driving the crack, thus contributing to enhancement of notch fatigue strength.

Accession For	
NTIS GRA&I	
DDC TAB	
Unannounced	
Justification	
By	
Distribution/	
Availability Codes	
Dist.	Avail and/or special
A	

Accession For	
NTIS GRA&I	
DDC TAB	
Unannounced	
Justification	
By	
Distribution/	
Availability Codes	
Dist.	Avail and/or special
A	

UNCLASSIFIED

SECURITY CLASSIFICATION OF THIS PAGE (When Data Entered)

TABLE OF CONTENTS

	Page
LIST OF FIGURES	iii
LIST OF TABLES	iv
LIST OF ABBREVIATIONS	v
ABSTRACT	1
ADMINISTRATIVE INFORMATION	1
INTRODUCTION	2
BACKGROUND	2
APPROACH	3
RESIDUAL STRESS ANALYSIS	3
FATIGUE TESTS	5
RESULTS AND DISCUSSION	6
SUMMARY	9
REFERENCES	31

LIST OF FIGURES

1 - Profile of Notch Used in the Residual Stress Analysis and Fatigue Tests of Inconel 718	10
2 - Slip-Line Field for Wedge Indentation as Described by Grunzweig et al	11
3 - Penetration Depth Versus Notch Rolling Load on a 0.560-Inch-Diameter Specimen of Inconel 718 Using Notch Rollers of Different Root Radii	12
4 - Slip-Line Field for a Semicylindrical Cavity	13
5 - Slip-Line Field for Modeling the Notch Indentation Process	14
6 - Finite-Element Map Used for "Loading"	15
7 - Yielding Surface for Inconel 718	16
8 - Stress-Strain Curve for Inconel 718	17
9 - Yield Surface for Inconel 718 with Reduction from Full Elastic	18
10 - Finite-Element Map Used for Elastic "Unloading"	19
11 - Stress from Loading and Unloading Along the Notch Centerline	20
12 - Rotating Cantilever-Beam Fatigue Specimen Before Notching	21
13 - Notch Roller Employed in Fatigue Tests	22
14 - Rolled Notch Depths for Hybrid Specimens	23

	Page
15 - Metal State Resulting from Notch Rolling	24
16 - Predicted Residual Stresses in the x Direction Resulting from Notch Rolling	25
17 - Predicted Residual Stresses Resulting from Notch Rolling	26
18 - Results of Rotating Cantilever-Beam Fatigue Tests of Inconel 718 with Machined and Rolled Notches	27
19 - Fracture Surfaces of Machined and Rolled Notched Fatigue Specimens	28
20 - Photomicrograph of Cross Section of a Rolled Notch in a Round Specimen (0.560-in. diameter) of Inconel 718	29
21 - Photomicrograph of the Notch Cross Section Showing the Notch Root Fatigue Crack and the Fatigue Crack Which Caused Failure	30

LIST OF TABLES

1 - Mechanical Properties and Chemical Compositions of Inconel 718	6
2 - Summary of Hybrid Specimen Fatigue Test Results	8

LIST OF ABBREVIATIONS

AC	Air cooled
°C	Degrees Celsius
FC	Furnace cooled
ksi	Thousand pounds per square inch
mm	Millimeters
MPa	Megapascals
wt %	Weight percent

ABSTRACT

The effects of cold forming on the fatigue behavior of threads were analyzed using slip-line field and finite-element analyses. Bolt threads were simulated using notched rotating cantilever-beam fatigue specimens of Inconel 718. The slip-line fields for wedge indentations, with some modifications, were used to analyze the deformation process of notch rolling. Stresses on the deepest slip lines were used in an elastic finite-element analysis of the internal stresses existing outside the slip-line field during deformation.

Negatives of the loads on the notch surface from the indenter were used in a second elastic finite-element analysis to determine the internal stresses from unloading. These two stress analyses, with a correction for yielding, were employed to map the residual stress distribution around the rolled notch. The predicted residual stress distribution showed an intense compressive region below the notch root. However, a short distance away from and to the side of the notch, there began a region of residual tensile stresses.

This stress distribution was then used to rationalize the fatigue crack propagation behavior of Inconel 718 rotating cantilever-beam fatigue specimens with rolled and machined notches. When specimens with machines notches were fatigue tested, the crack propagation direction was perpendicular to the axis of rotation and in the direction of the maximum alternating stress gradient. In the presence of a rolled notch the crack propagation path was altered to a direction 50° from the perpendicular to the axis of rotation. This change was attributed to the residual stress distribution around the notch as indicated by the stress analysis. This change in the direction of crack propagation also reduced the magnitude of the alternating stresses driving the crack, thus contributing to enhancement of notch fatigue strength.

ADMINISTRATIVE INFORMATION

This report was prepared as part of the Surface Ship and Craft Materials Block Program under the direction of Dr. H.H. Vanderveldt, Naval Sea Systems Command (SEA 05R15). The effort was supervised by Mr. John Gudas, David W. Taylor Naval Ship Research and Development Center (Code 2814) under Center Project 2803-160, Element 62761N.

Portions of this study were sponsored by the Naval Sea Systems Command (Sea 05R13) and were performed under Work Unit 2814-181, Task Area 50379, SL001, Task 19979. The program manager was Mr. C. Miller (SEA 05R13).

INTRODUCTION

All machinery systems with notched or threaded members have potential fatigue problems. In some systems where these conditions cannot be alleviated with redesign or material substitution, certain changes in fabrication techniques may provide an increase in fatigue resistance. One such technique is notch rolling, which has long been used as a fatigue prevention method, especially in the fasteners industry. The actual mechanism leading to this enhanced fatigue resistance of rolled-over machined notches is not clearly defined. The purpose of this investigation was to develop a better understanding of the residual stress pattern around a rolled notch and its effects on fatigue crack initiation and growth.

Residual stresses occur when a portion of a piece of metal experiences plastic flow and the remainder of the material experiences only elastic strains. In the particular case of notch rolling, the metal is deformed by a notch roller which causes plastic flow of the metal around the notch and sets up the residual stresses. An analytical tool which might give the residual stresses for this problem would be one of the new finite-element programs which could treat plasticity. This approach to the problem employed the more traditional tools of slip-line field theory for the plastic analysis and elastic finite-element analysis for the elastic portion of the problem. With appropriate merging of the two solutions, a stress map resulting from the notch rolling of the material was obtained. A second finite-element program was used to characterize the stresses resulting from the elastic unloading of the notch as the roller was removed. The solutions were combined to describe the residual stress distribution around the notch, which was then used to analyze the fatigue behavior of notched specimens.

BACKGROUND

The beneficial effects of surface rolling on fatigue resistance were first investigated by Foppl.^{1*} Later work by Horger² on the effects of surface rolling indicated that increased fatigue strength resulted principally from strain hardening of the surface layer. Further support of this view was given by Frost³ who showed a 43-percent increase in fatigue strength of mild steel by uniform cold work.

Although the surface strain hardening rationale may be applicable to surface rolling, the fatigue behavior of notched specimens requires a different explanation. As in the case of surface rolling, notch rolling results in an increase in fatigue strength compared to cut or ground notches and threads. Field⁴ found a 200-percent increase in the fatigue strength of rolled threads over

*A complete listing of references is given on page 31.

ground threads for 3/4-in. steel studs. Bellow and Faulkner⁵ found increases in fatigue strength of 66 and 51 percent for rolled threads over cut threads tested in air and saltwater, respectively. A study of the fatigue of prestressed notches by Fuchs⁶ concluded that prestressing had its most significant effect on fatigue crack growth and little effect on fatigue crack initiation. Fatigue crack growth requires cyclic tensile stresses ahead of the crack⁷ which are attenuated by the presence of residual compressive stresses near the notch root. Fatigue crack initiation requires slip produced by cyclic shear stresses⁷ which are enhanced by the notch through its stress concentration factor and not affected by the residual stresses. Fuchs⁶ investigated this model by examining prestressed notched aluminum alloy fatigue specimens which were removed from test at various cyclic lives before failure occurred. Examinations of these fatigue specimens indicated that nonpropagating fatigue cracks would initiate within 1/2 million cycles but not extend even after an additional 5 million cycles. The existence of nonpropagating fatigue cracks resulting from rolled notches was also suggested by Frost et al.⁸ From these results it appears that the compressive residual stresses around the rolled notch are responsible for the beneficial effects of rolling on fatigue resistance of notched specimens.

APPROACH

The objective of this investigation was to characterize the residual stresses near a circumferential notch, shown in Figure 1, with a stress concentration factor of 3.26. The notch was rolled into a round rotating cantilever fatigue specimen of Inconel 718, and the analysis related the residual stresses to the material's notched fatigue behavior. The investigation consisted of two phases, including the residual stress analysis and the analysis of the notch fatigue tests performed on rotating cantilever-beam specimens of Inconel 718.

RESIDUAL STRESS ANALYSIS

The analysis for residual stresses was comprised of two segments — calculating the stress field resulting from the notch formation, and calculating the stresses resulting from the elastic unloading of the notch surface. The two stress fields were then superimposed, with the sum of the two being the residual stresses. The two main assumptions made for the residual stress analysis were that an axisymmetric problem could be approximated with a two-dimensional plane strain solution, and that the stresses on the deepest slip lines of a slip-line field solution could be used to find the loads on the elastic substrate surrounding the deformed metal of the notch.

The notch indentation process with a sharp wedge was examined by Grunzweig et al.⁹ using their slip-line field shown in Figure 2. It was shown that during the indentation process, while the coronet was being formed, a linear relationship existed between the load on the wedge indenter and the depth of penetration. A linear relationship also existed for the notch rolling process as shown in Figure 3, which is a plot of the notch rolling load versus depth of penetration using two notch rollers with different root radii on a 0.560-in. diameter specimen of Inconel 718. The notch roller with the sharper root radius produced a greater penetration depth for the same load. However, both curves had the same slope, indicating that the variations between the curves resulted from different behaviors in the very early stages of notch formation (the detection of which was beyond the sensitivity of the instruments used). Similar results were found by Johnson et al.¹⁰ when using wedges with sharp and flat edges. Although the wedge indentation model of Grunzweig et al.⁹ may predict the proper overall behavior, any load prediction obtained with a wedge indentation model would yield smaller than realistic loads for the notch indenter with a 0.010-in. tip radius for a given penetration.

The Hill slip-line field solution, Figure 4, for a semicylindrical cavity expanded in a plane surface¹¹ which was used to account for the radius at the indenter tip was combined with the wedge indentation slip-line field to produce a slip-line field for notch rolling, Figure 5. Since the experimental deformation was accomplished using a lubricated roller, which can be considered similar to the wedge indenter experiencing a to-and-fro motion as reported by Grunzweig et al.,⁹ the process was assumed nearly frictionless. The calculated stresses across the deepest slip line were used as the applied loads for the finite-element computer program which only modeled the material below the slip-line field, Figure 6. The finite-element program (obtained from the Civil Engineering Department at the University of Pittsburgh) modeled an area 0.40 in. (10.16 mm) * by 0.28 in. (7.11 mm) with 294 nodes and 511 elements. The stresses were transformed into loads acting on the nodal points of the loaded boundary. It was assumed that there were zero strains acting across the notch centerline and the centerline of rotation (the longitudinal direction). The area of the finite-element map was approximately 70 times that of the slip-line field to assure the needed constraint for a realistic model. The output of the finite-element computer program was the tensile stresses in the longitudinal and transverse directions (σ_x and σ_y), shear stresses (τ_{xy}), and the principal stresses (σ_1 , and σ_2) for all the elements.

The stresses of some of the elements around the notch were above the yield stress of Inconel 718. These stresses were corrected using the quadratic yielding equation for plane strain,¹² Figure 7, and the stress-strain curve for Inconel 718, Figure 8. These two graphs were

*Definitions of abbreviations used are given on page v.

used to construct a second yielding surface, Figure 9, which was employed to compute the stress reduction percentage applied to elastic finite-element results to account for yielding. Although the corrections were usually small, their existence meant that the slip-line field should have been slightly deeper, especially near the notch root. The analysis also revealed a small "dead-metal cap" at the root of the notch. The abovementioned corrections were also calculated using the quadratic equation for plane stress,¹² Figure 7, which resulted in slight differences in stresses from the plane strain analysis except for the dead-metal cap which disappeared. The plane strain corrected finite-element output gave the stress map of the material at the completion of the notch rolling.

The second phase of the residual stress analysis dealt with the elastic unloading of the notch surface. This finite-element program had 317 nodes and 551 elements, most of which were identical to those of the previously mentioned finite-element analysis. This analysis required a finite-element map of the entire area including the plastically deformed area around the notch, and the loads applied to the inner surface of the notch by the indenter at the final instant of rolling, Figure 10. Again, the slip-line field was used to calculate the stresses on the notch surface which were transformed to nodal point loads for the finite-element program. Since this phase was to model the assumed elastic unloading of the notch, the negatives of the applied indenter loads were used in the computer program. The centerline boundary conditions were the same as in the loading analysis. The output of the second finite-element analysis was the internal stresses resulting from the elastic unloading of the notch surface at the end of the notch rolling process.

The two finite-element maps were then superimposed and the stresses of the corresponding elements were summed, producing the residual stress distribution.

Figure 11 is a plot of the stresses acting across the notch centerline as a function of their location along the notch centerline for the loading and unloading situation. Also, Figure 11 shows the results of the loading analysis without the yielding correction. The sum of the loading and unloading curves would produce the residual stress distribution acting across the notch centerline.

FATIGUE TESTS

The fatigue tests were performed on Inconel 718 bar in the fully heat-treated condition with the properties shown in Table 1. The specimens used were rotating cantilever-beam specimens or McAdam specimens¹³ which had a 0.500-in. (12.7-mm) test diameter and an overall length of 11 in. (280 mm), as shown in Figure 12.

TABLE 1 — MECHANICAL PROPERTIES AND
CHEMICAL COMPOSITIONS OF INCONEL 718

Tensile Stress	258.9 ksi (178 MPa)
Yield Stress	178.6 ksi (123 MPa)
Elongation (% in 2 in.)	17
Chemical Composition (wt %)	
Ni	53.3
Cr	18.0
Fe	18.2
Mo	3.0
Co	3.3
Heat Treatment	Annealed and hot rolled (1700° to 1800°F) then aged (1325°F/8 hr, FC to 1150°F, hold at 1150°F/8 hr, AC)

The specimens were dead-weight loaded and rotated at 1725 rpm until failure, which was defined as a complete separation of the specimen. The rolled notches were formed with a hydraulically actuated notch roller attached to a lathe bed. While the specimen was rotating in the lathe, hydraulic pressure was gradually increased until the proper notch depth was achieved.

The notches had a depth of 0.031 in. (0.787 mm) with a 0.010-in. (0.25-mm) root radius and a total notch angle of 45°, Figure 13. The rolled notches differed slightly from the machined notches due to the coronet of metal pushed up on both sides of the rolled notch. Nine specimens were tested (five with rolled notches, four with machined notches) in air at various stress levels.

In addition to the nine smooth and notched specimens, four hybrid specimens were tested at a stress level of ± 40 ksi (276 MPa) in air. The hybrid specimens were produced by rolling notches to depths of 0.007 to 0.025 in. (0.18 to 0.63 mm) and then machining them all to some final notch profile as in Figure 14.

RESULTS AND DISCUSSION

The results of the first finite-element analysis for the stress field resulting from the notch formation are shown in Figure 15. The three areas shown are: the fully plastic area, which was slightly larger than the original slip-line field; the elastic region comprising most of the area; and

the transitional region between the two, which had stresses above the elastic limit but less than the engineering yield stress.

The sums of the stresses acting in the longitudinal direction obtained from the superposition of the two finite-element programs are shown schematically in Figure 16. The region marked "compression" contains all the elements which had a residual compressive stress acting in the longitudinal direction. The magnitude of these stresses was greatest near the surface of the notch and went to zero at the boundary between the compressive and tensile region. In the region of residual tension the stress magnitude increased for elements further below the boundary, through a maximum and then approached zero. The distribution of longitudinal stresses acting on the notch centerline is shown in Figure 17.

The results of the fatigue tests performed on the Inconel 718 with machined and rolled notches are shown in Figure 18. These results clearly show the enhanced fatigue resistance resulting from notch rolling compared to machined notches with the same stress concentration factor, $K_t = 3.26$. The compressive residual stress region around the notch root accounts for the greater fatigue resistance of the rolled notches over the machined notches. This residual stress configuration makes it very difficult for a crack to grow from the notch root down the notch centerline since crack growth would require very high cyclic tensile stresses to counteract the mean compressive stress. The normal crack extension path in bending or axial fatigue with a machined notch assuming cyclic stresses applied in the longitudinal (x) direction, perpendicular to the notch centerline, is along the notch centerline. Such a fracture surface for a machined notched Inconel 718 fatigue specimen is shown on the left in Figure 19. Also shown in Figure 19 is a failed specimen with a rolled notch. The orientations of the fatigue cracks are very different despite the identical loading conditions of the two specimens. This fatigue crack behavior was also seen by Shatinskii¹⁴ on notched steel fatigue specimens. The different crack orientation on the rolled specimens resulted from the residual stress distribution around the notch root. The compressive residual stresses below the notch root made fatigue crack growth difficult by superimposing a large mean compressive stress on cyclic stresses experienced by the metal. The path taken by the fatigue crack, which is 50° from the notch centerline, allowed the crack tip to grow into a field of residual tension near the notch root, as shown in Figure 17. After the fatigue crack was initiated via the shear stresses, the crack was able to propagate into this field of residual tension. The applied cyclic stresses on the crack path, which were attenuated but still possessed tensile components, coupled with a mean tensile stress provided the tensile cyclic

stresses needed for fatigue crack growth. The residual stresses on the fatigue crack shown in Figure 17 had a compressive stress region adjacent and beyond the tensile region. Once the crack has grown through the residual tensile stress region, this compressive stress region should nearly disappear as the constraint and balancing tensile field is reduced. At some point away from the influence of the rolled notch, the crack front should change direction and grow toward the center of the specimen. This was observed in tests and is shown in Figure 19.

The four hybrid specimens tested with an applied alternating stress of ± 40 ksi (276 MPa) displayed fatigue lives greater than 10^8 cycles. The notch rolled-only specimens tested at the same stress level failed at 8×10^6 cycles. The fatigue strength of the hybrid specimens apparently resulted from the final notch machining which removed any surface asperities produced by the notch rolling process. Such an asperity, which would act as a local stress raiser causing early crack initiation, is shown in Figure 20. The hybrid fatigue specimens were removed from test after 10^8 cycles and underwent a heat tinting process of 1 hr at 700°F (371°C) which changed the specimen's surface color from silver to light straw. Three of the four specimens were then retested with an applied alternating stress of ± 65 ksi (448 MPa) until failure, as summarized in Table 2. The fatigue strengths of the hybrid specimens indicated that the residual compressive stress region below the notch root exists to a depth of at least 0.024 in. (0.61 mm) since specimen A, with the shallowest rolled notch of four hybrid specimens (A, B, C, and D), was a run out (10^8 cycles) at ± 40 ksi (276 MPa).

TABLE 2 — SUMMARY OF HYBRID SPECIMEN FATIGUE TEST RESULTS

Specimen Designation	Depth of Notch Rolling in. (mm)	Final Notch Depth after Machining in. (mm)	Cycles at ± 40 ksi (± 276 MPa)	Cycles at ± 65 ksi (± 448 MPa)
A	0.007 (0.18)	0.031 (0.79)	10^8	1.9×10^7
B	0.013 (0.33)	0.031 (0.79)	10^8	1.8×10^7
C	0.019 (0.48)	0.031 (0.79)	10^8	8×10^6
D	0.025 (0.63)	0.031 (0.79)	10^8	Not tested

The fracture surfaces of specimens B and C appeared similar to those of the notch rolled-only specimens, as in Figure 19, with the fatigue crack which caused failure initiating away from

the notch root area. Also evident on the fracture surface of specimens B and C were fatigue cracks at the notch root which had heat tinted surfaces, indicating their existence before being subjected to the higher alternating stress of ± 65 ksi (448 MPa). The existence of these nonpropagating fatigue cracks at the notch root supports the previously mentioned work by Fuchs.⁶ Figure 21 is a photomicrograph showing the notch root fatigue cracks and the fatigue crack which caused the specimen failure. Figure 21 also indicated the presence of an area of compressive residual stresses below the notch root deterring fatigue crack propagation. The hybrid specimen A had a fracture surface similar to that of the machined notch fatigue specimen shown in Figure 19. The fracture surface had a heat tinted fatigue crack at the notch root which was similar in size to those in specimens B and C. However, the higher applied cyclic stress, 65 ksi (448 MPa), caused the fatigue crack to propagate out of the region of compressive residual stresses and fail the specimen, indicating a small zone of compressive residual stress.

SUMMARY

The fatigue behavior of notched specimens was investigated to understand the process which increases the fatigue resistance of rolled notches. The two phases of the investigation were the analytical prediction of the residual stress distribution from slip-line field theory and finite-element computer programs, and the analysis of notched fatigue data for Inconel 718 rotating cantilever fatigue specimens.

The investigation showed that a residual stress distribution can be constructed with a combination of slip-line field theory and elastic finite-element programs. This process was used to produce a residual stress distribution that could rationalize the fatigue behavior of Inconel 718 with rolled notches. The investigation showed that the increase in fatigue resistance of the rolled notch resulted from the residual stress distribution of compressive stresses around the notch root, which caused a change of crack orientation during the early stage of fatigue crack growth. This altered fatigue crack growth path experienced smaller cyclic tensile stresses than the normal crack path, thus reducing the fatigue crack growth rate of the specimens with rolled notches.

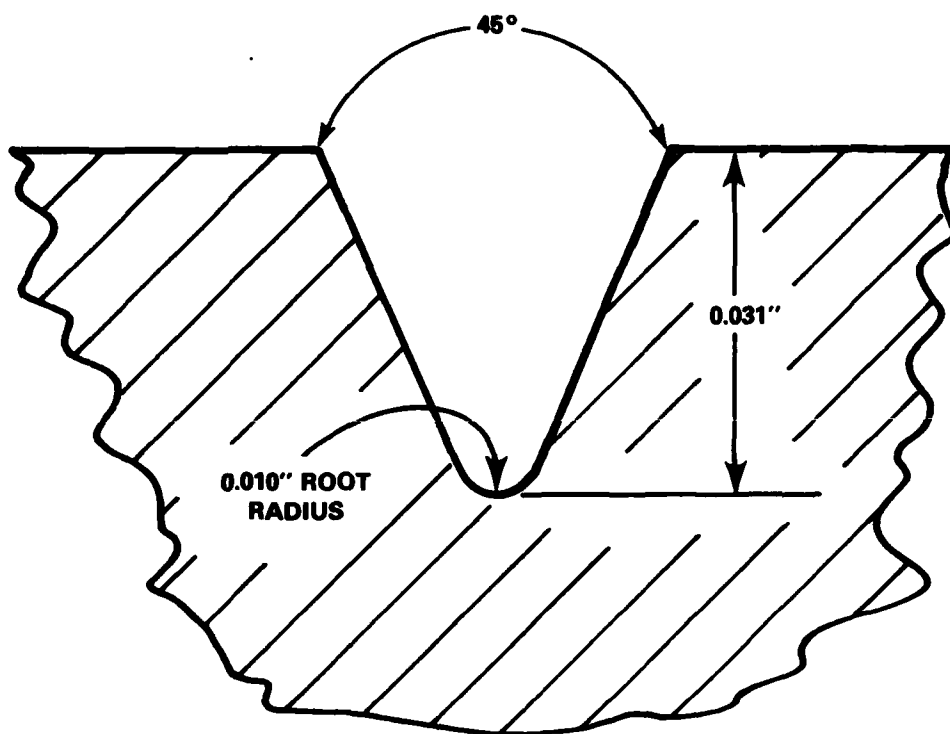


Figure 1 - Profile of the Notch Used in the Residual Stress Analysis and Fatigue Tests of Inconel 718

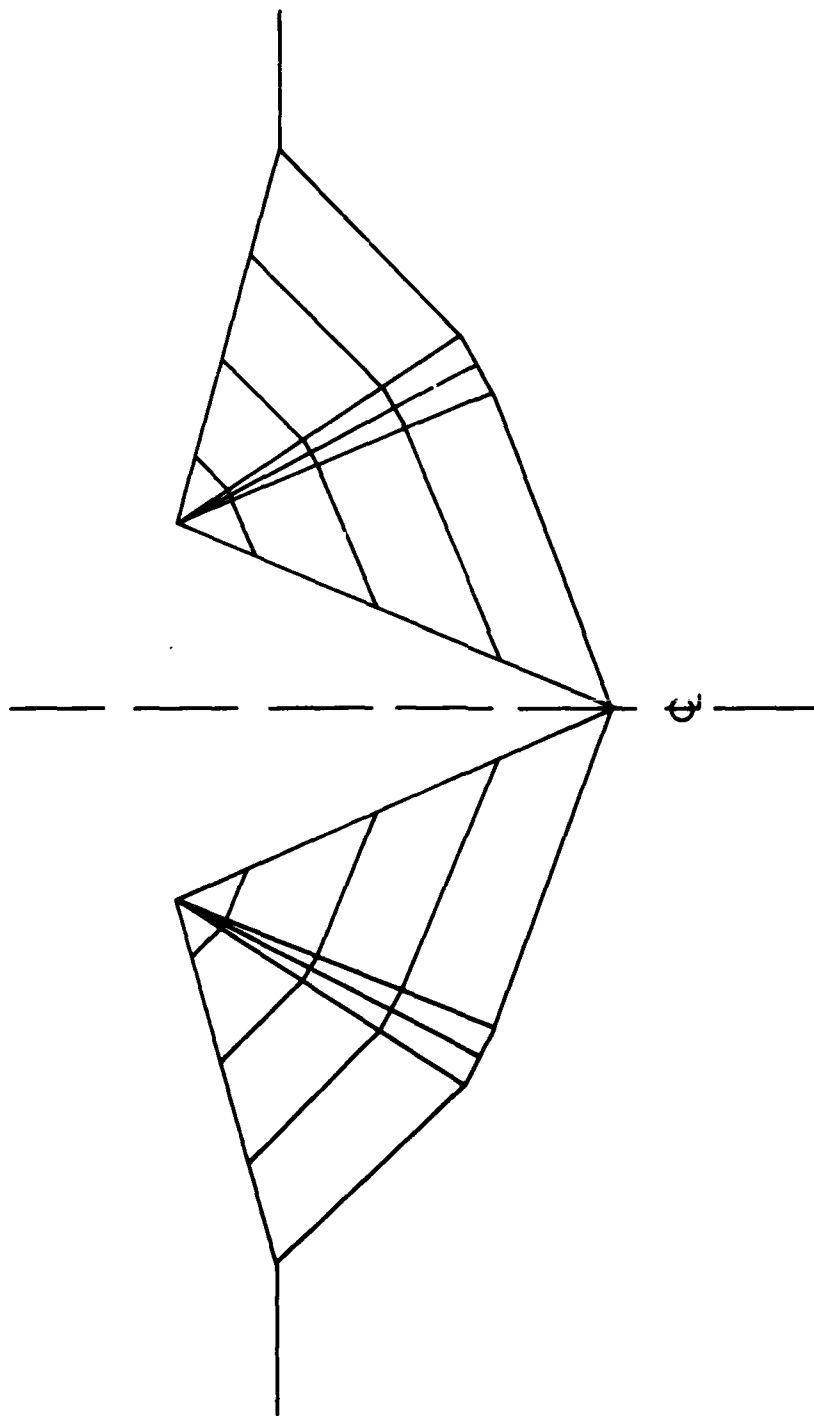


Figure 2 - Slip-Line Field for Wedge Indentation as Described by Grunzweig et al.⁹

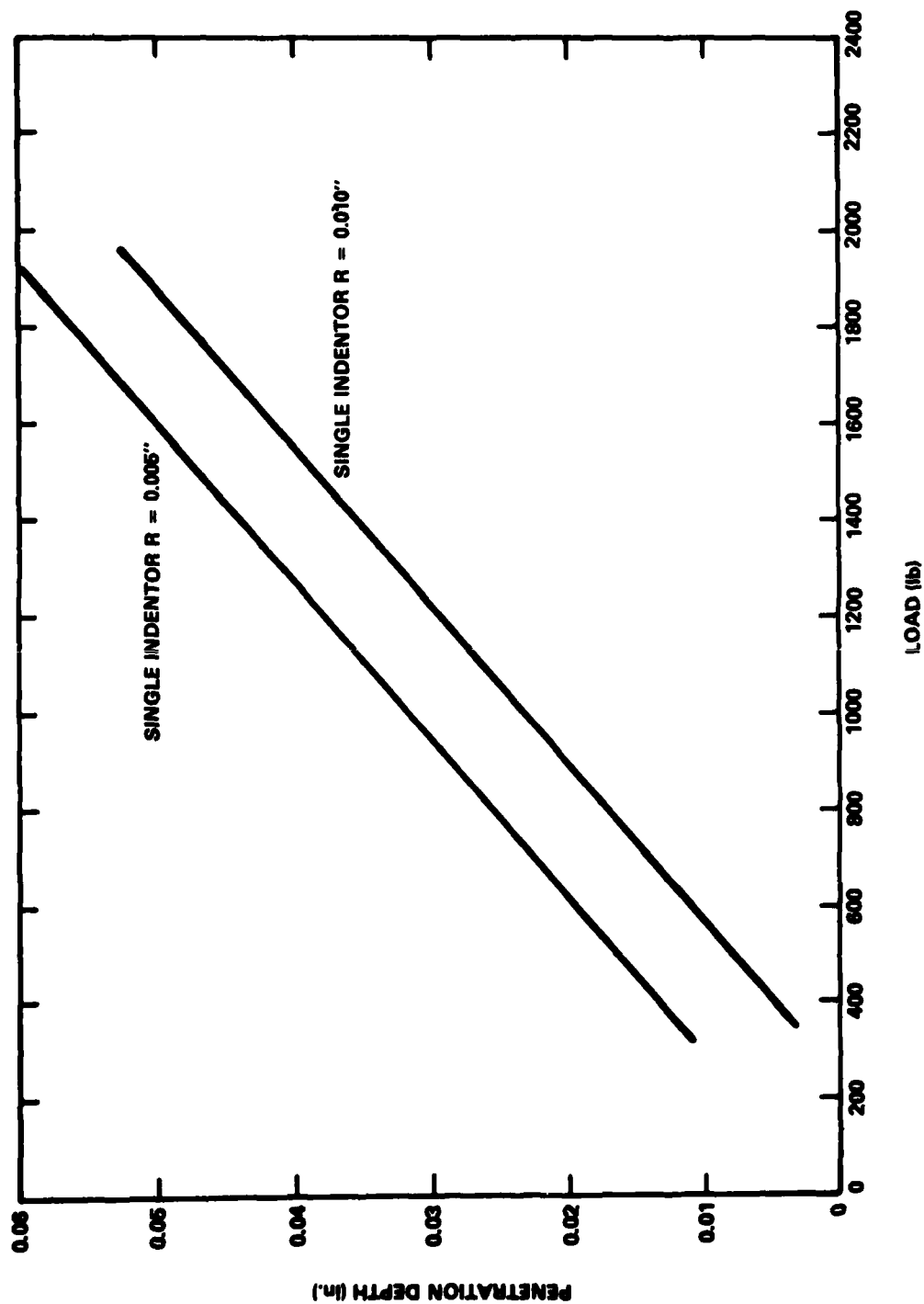


Figure 3 - Penetration Depth Versus Notch Rolling Load on a 0.560-Inch-Diameter Specimen of Inconel 718 Using Notch Rollers of Different Root Radii

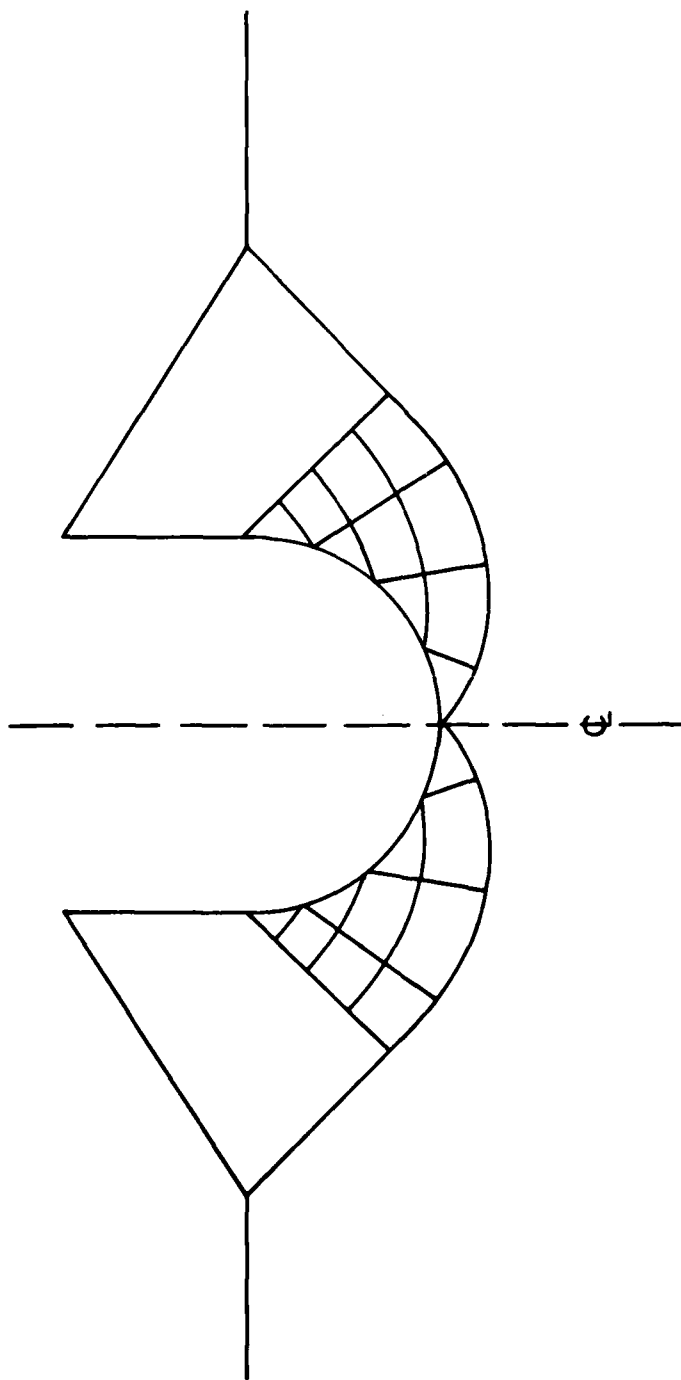


Figure 4 - Slip-Line Field for a Semicylindrical Cavity¹¹

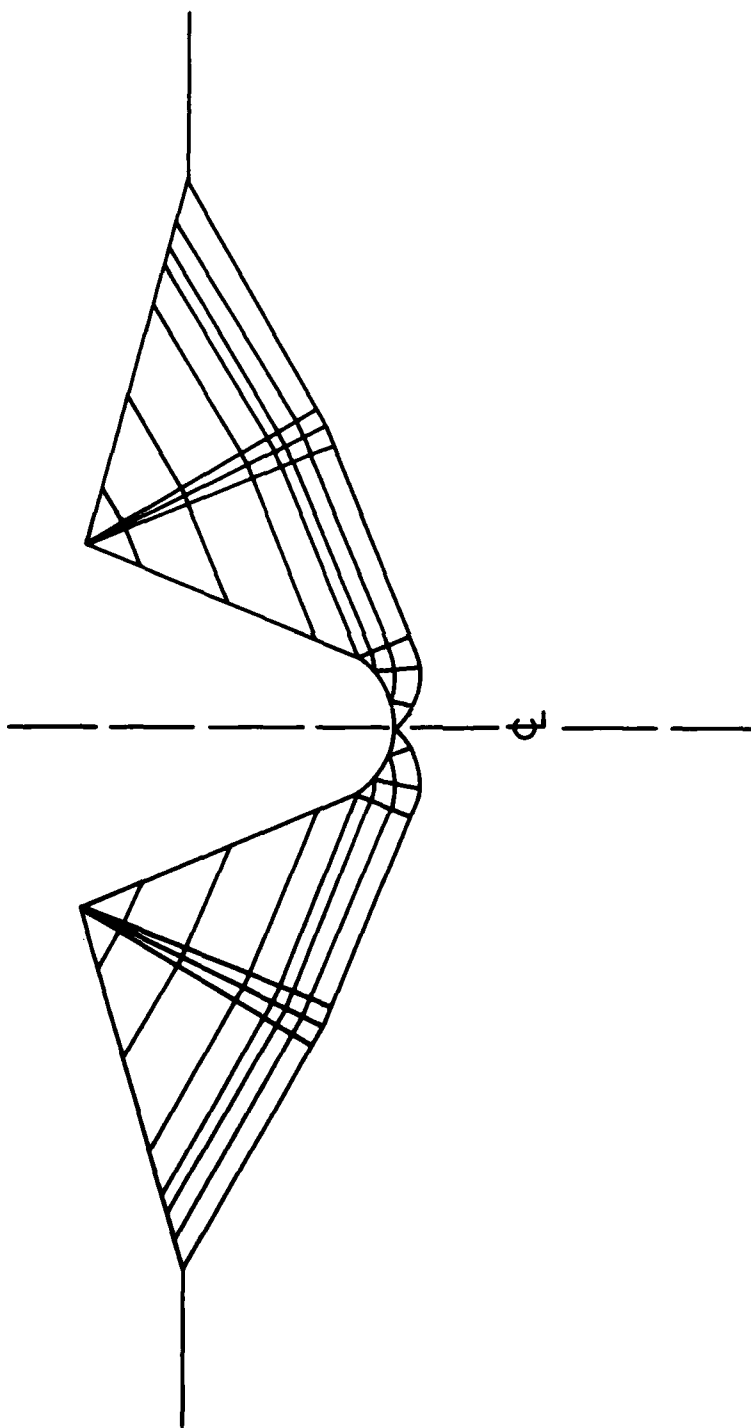


Figure 5 - Slip-Line Field for Modeling the Notch Indentation Process

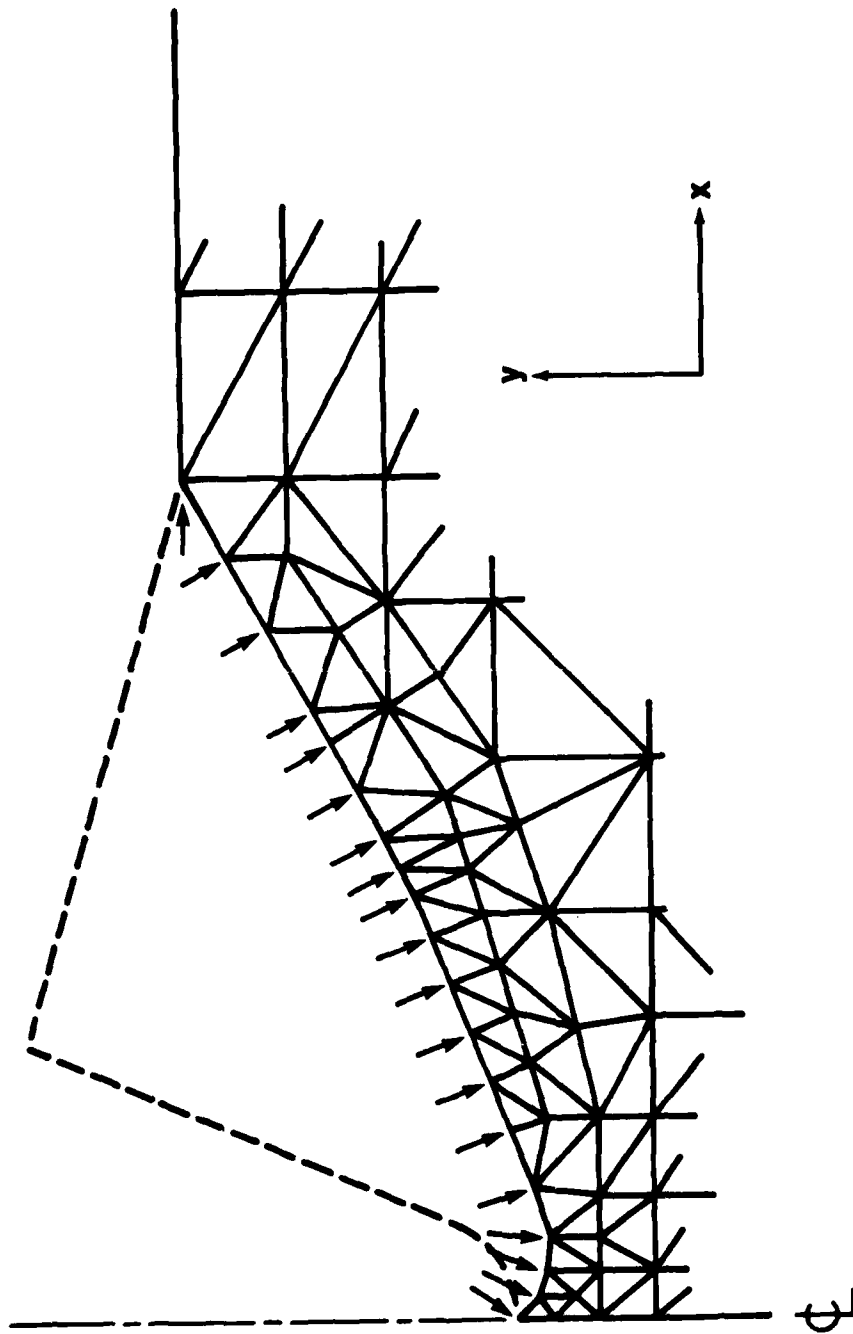


Figure 6 - Finite-Element Map Used for "Loading"

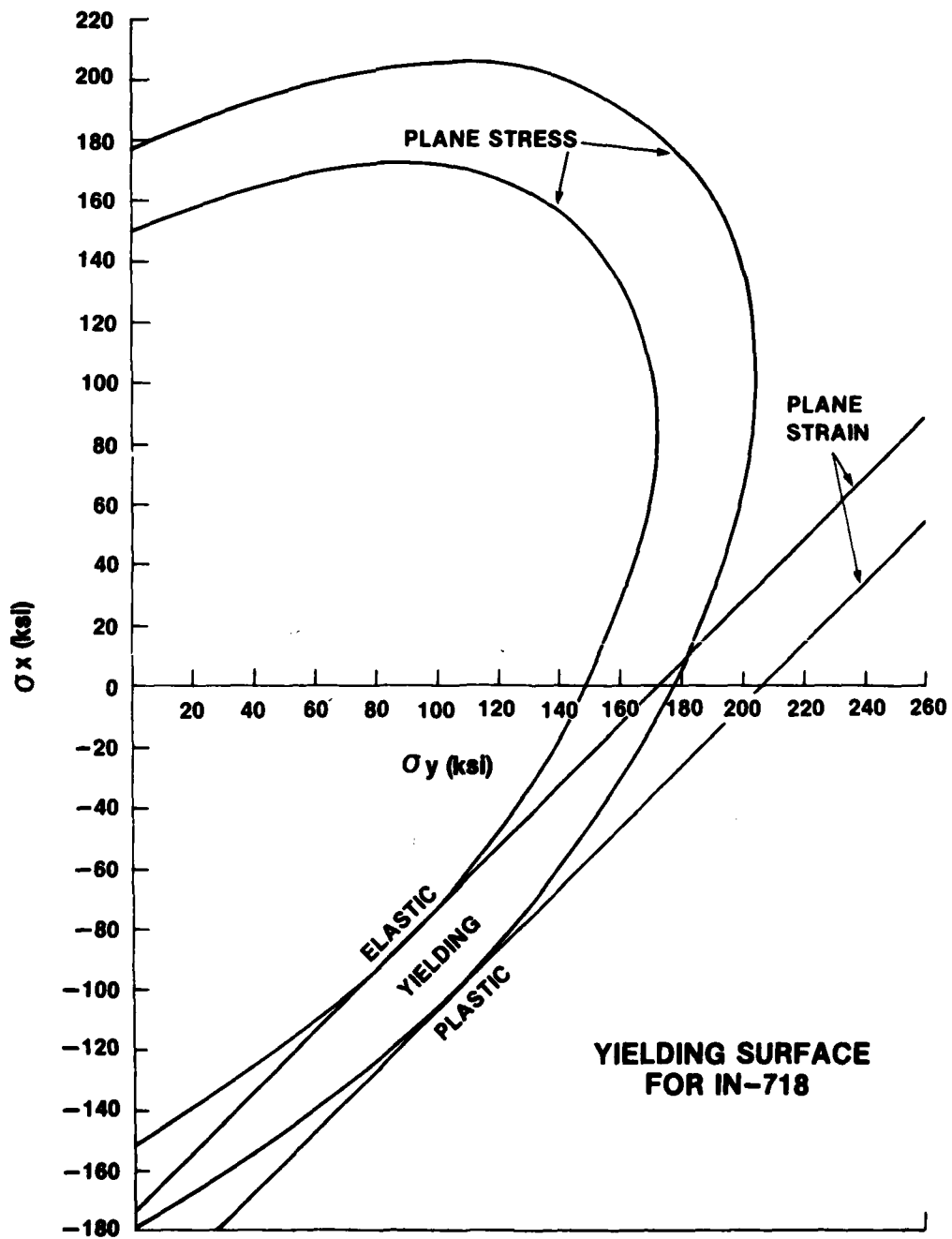


Figure 7 - Yielding Surface for Inconel 718

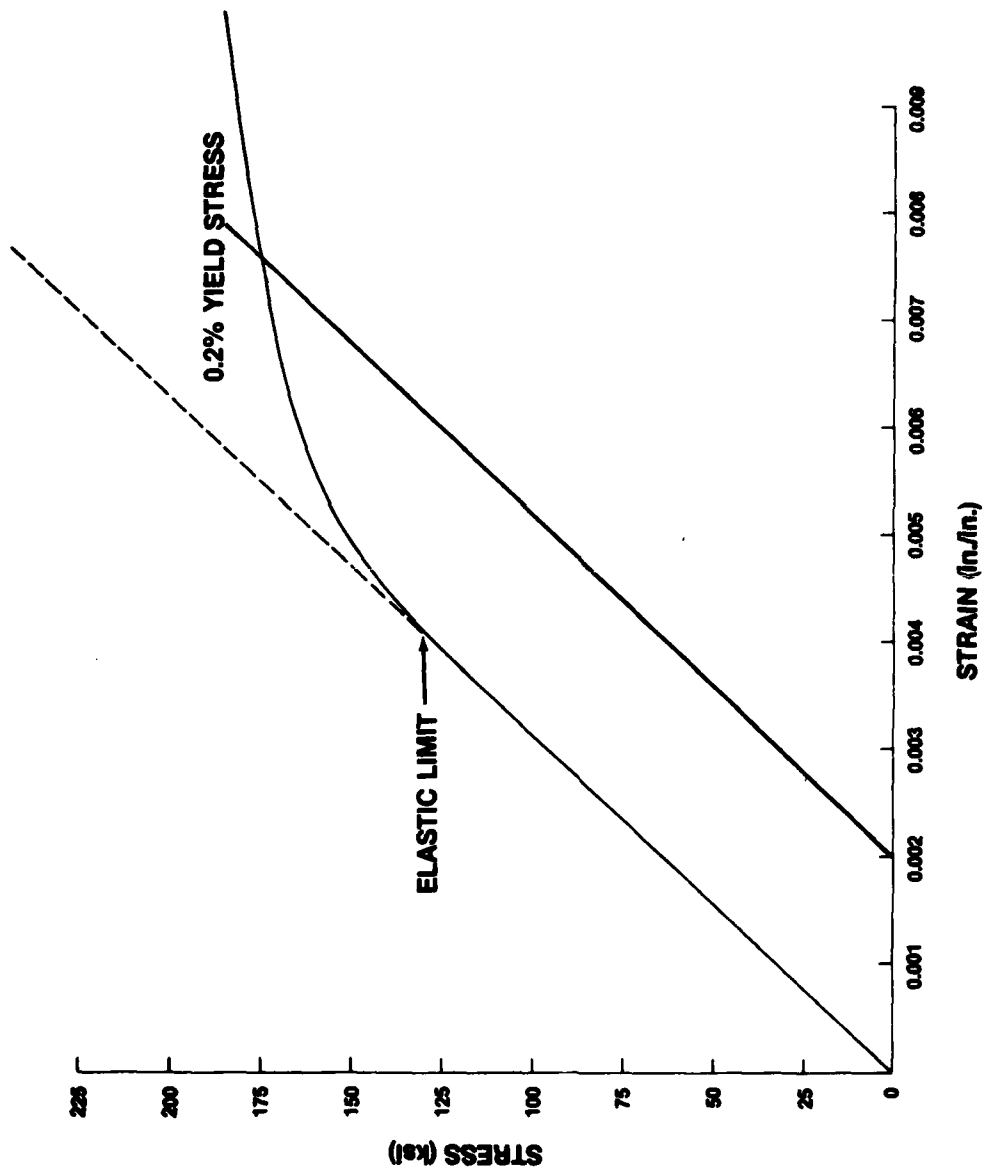


Figure 8 - Stress-Strain Curve for Inconel 718

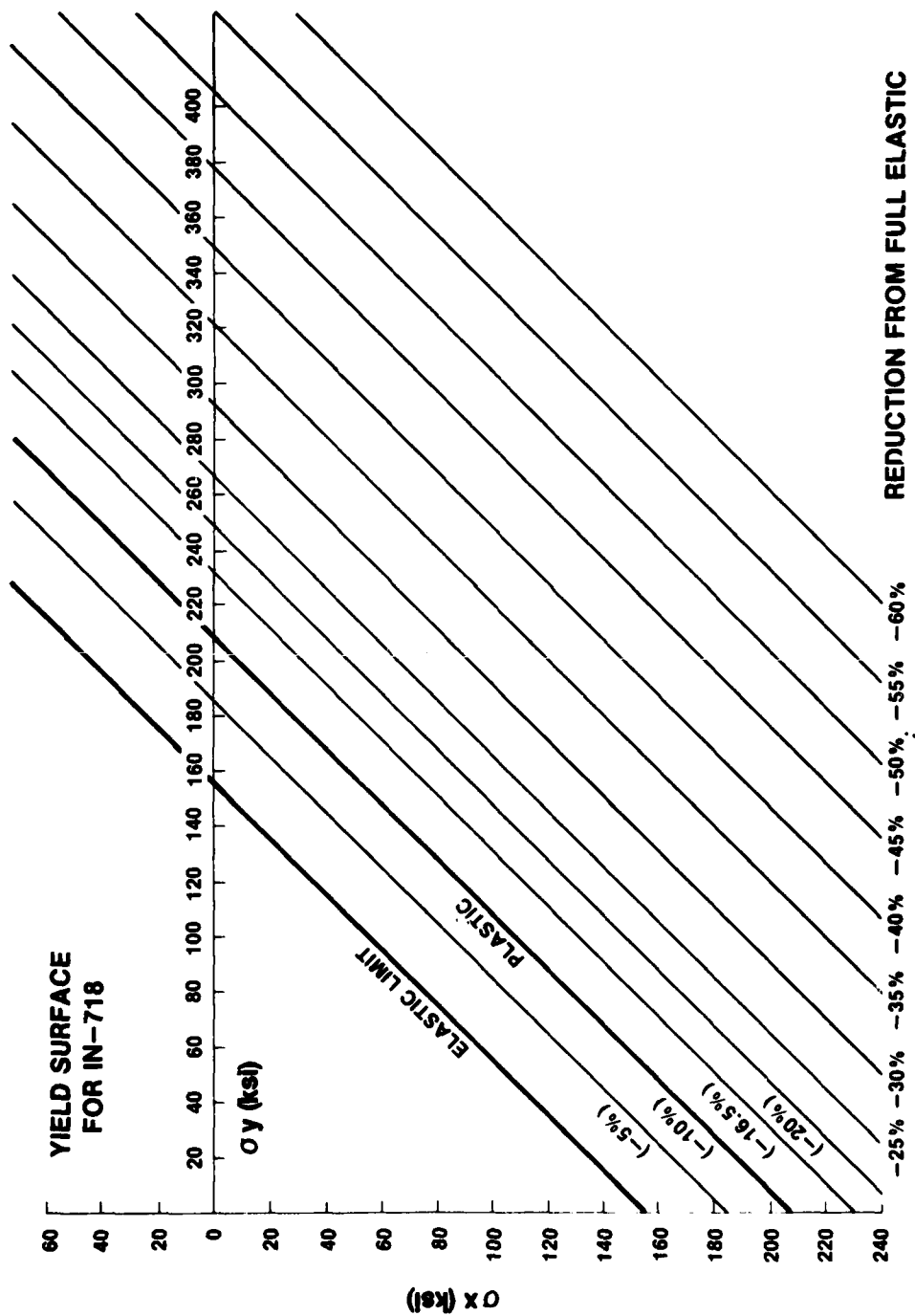


Figure 9 - Yield Surface for Inconel 718 with Reduction from Full Elastic

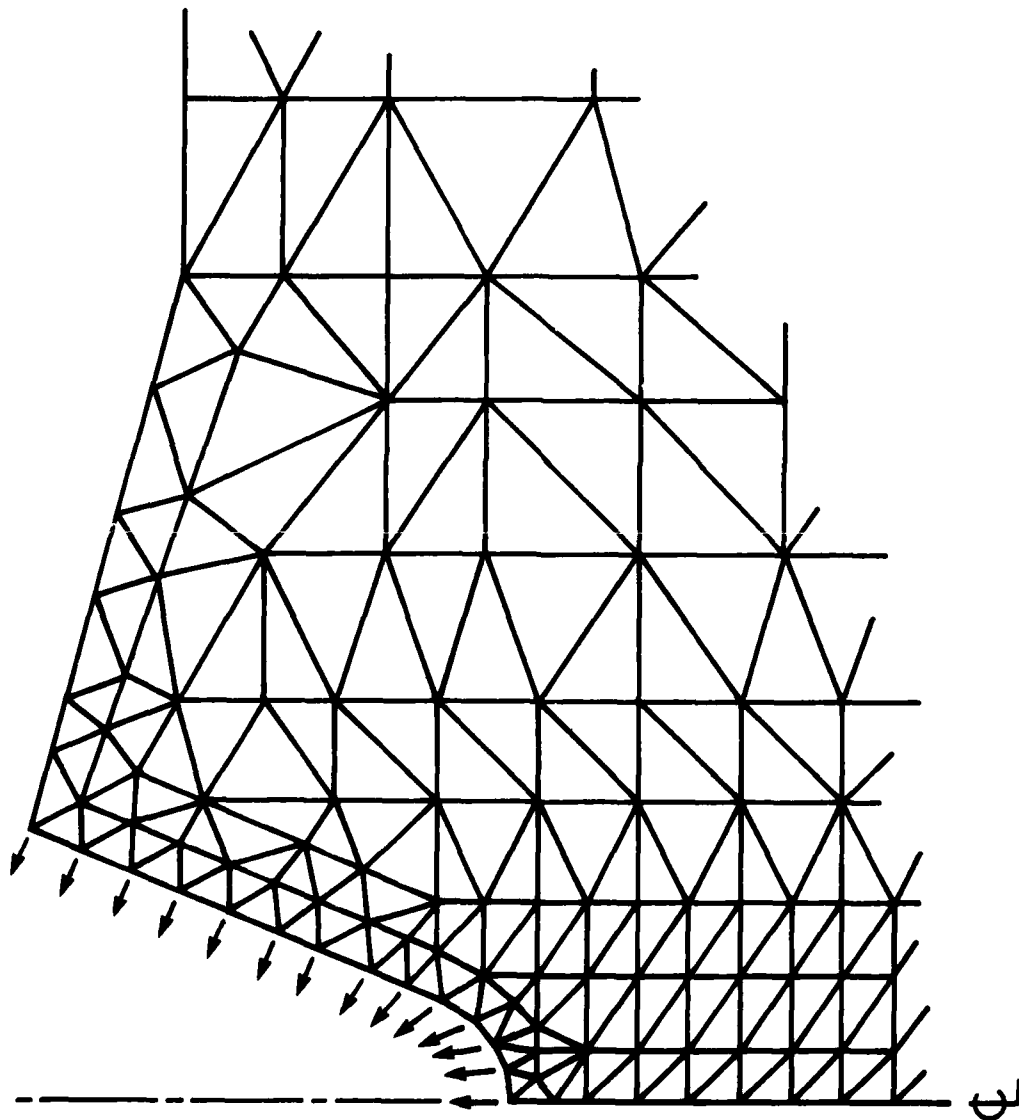


Figure 10 - Finite-Element Map Used for Elastic "Unloading"

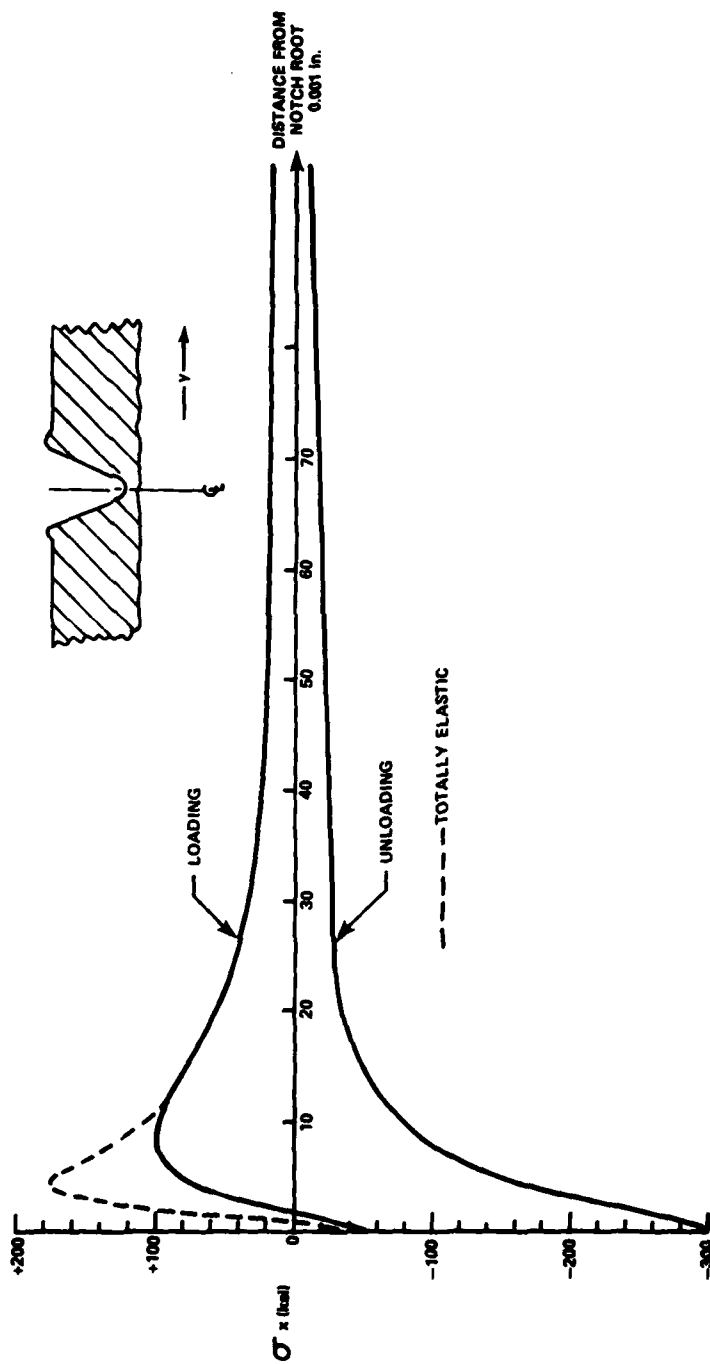
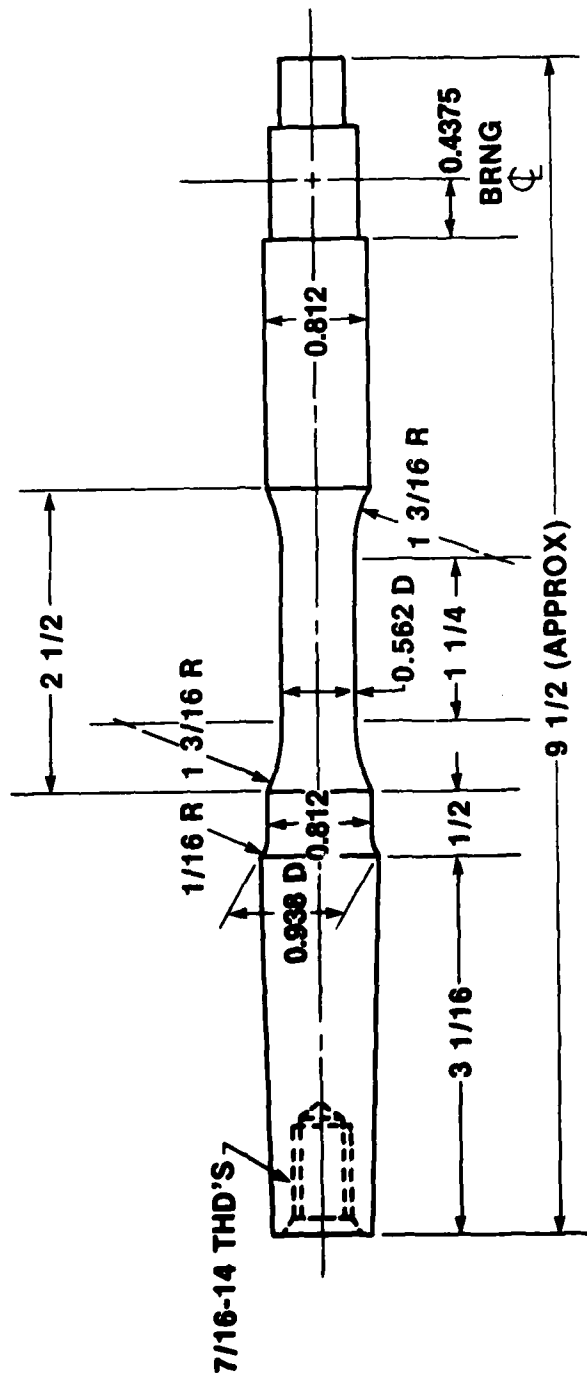
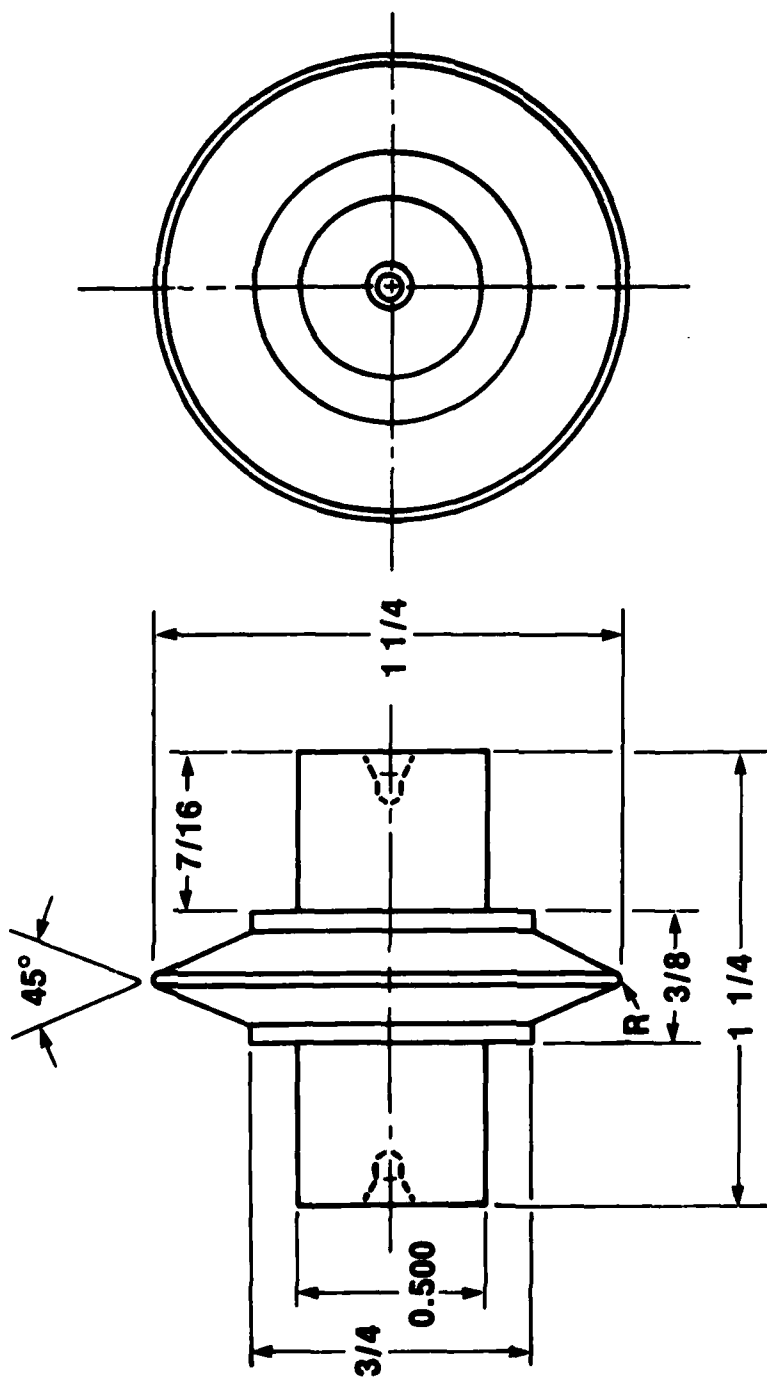


Figure 11 - Stress From Loading and Unloading Along the Notch Centerline



NOTE: DIMENSIONS IN INCHES.

Figure 12 - Rotating Cantilever-Beam Fatigue Specimen Before Notching



$R=0.010 \pm 0.001$

NOTE: DIMENSIONS IN INCHES.

Figure 13 - Notch Roller Employed in Fatigue Tests

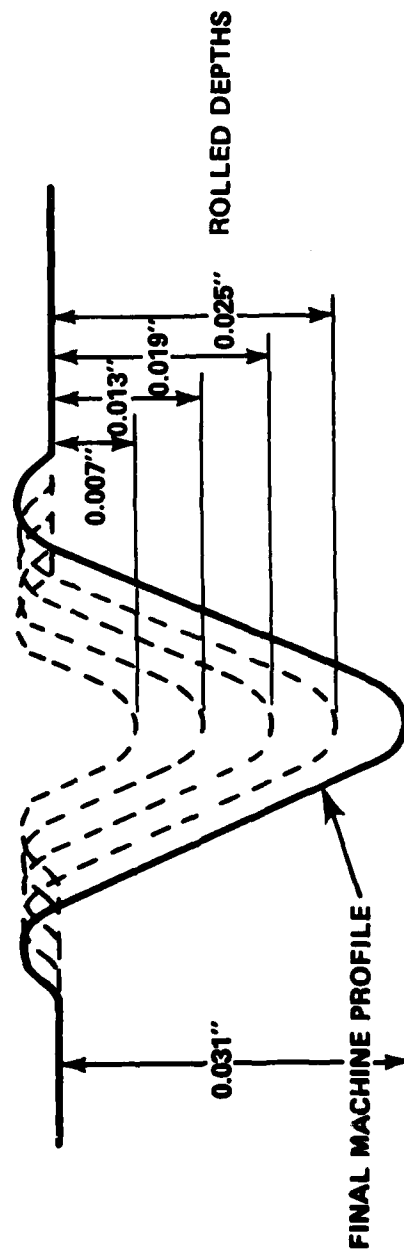


Figure 14 - Rolled Notch Depths for Hybrid Specimens

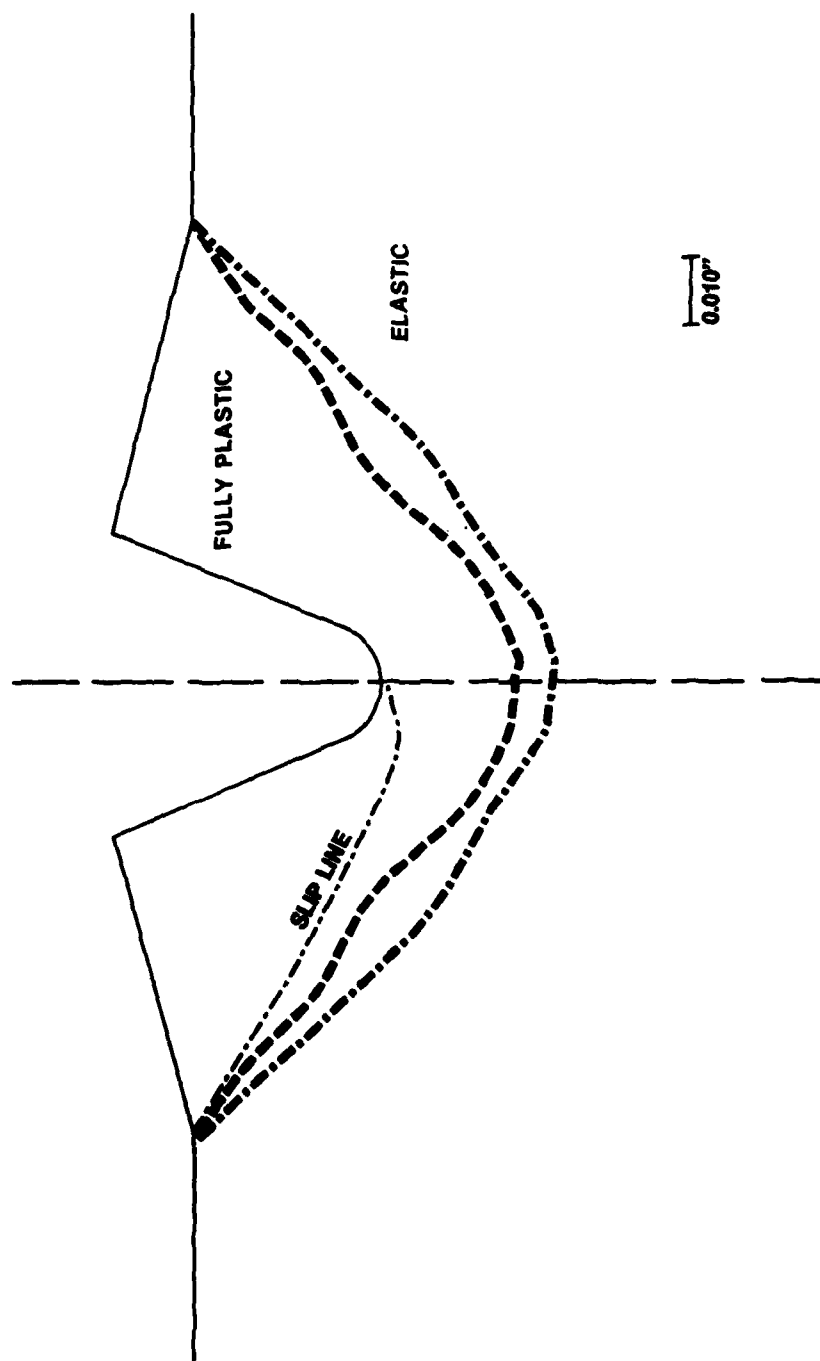


Figure 15 - Metal State Resulting From Notch Rolling

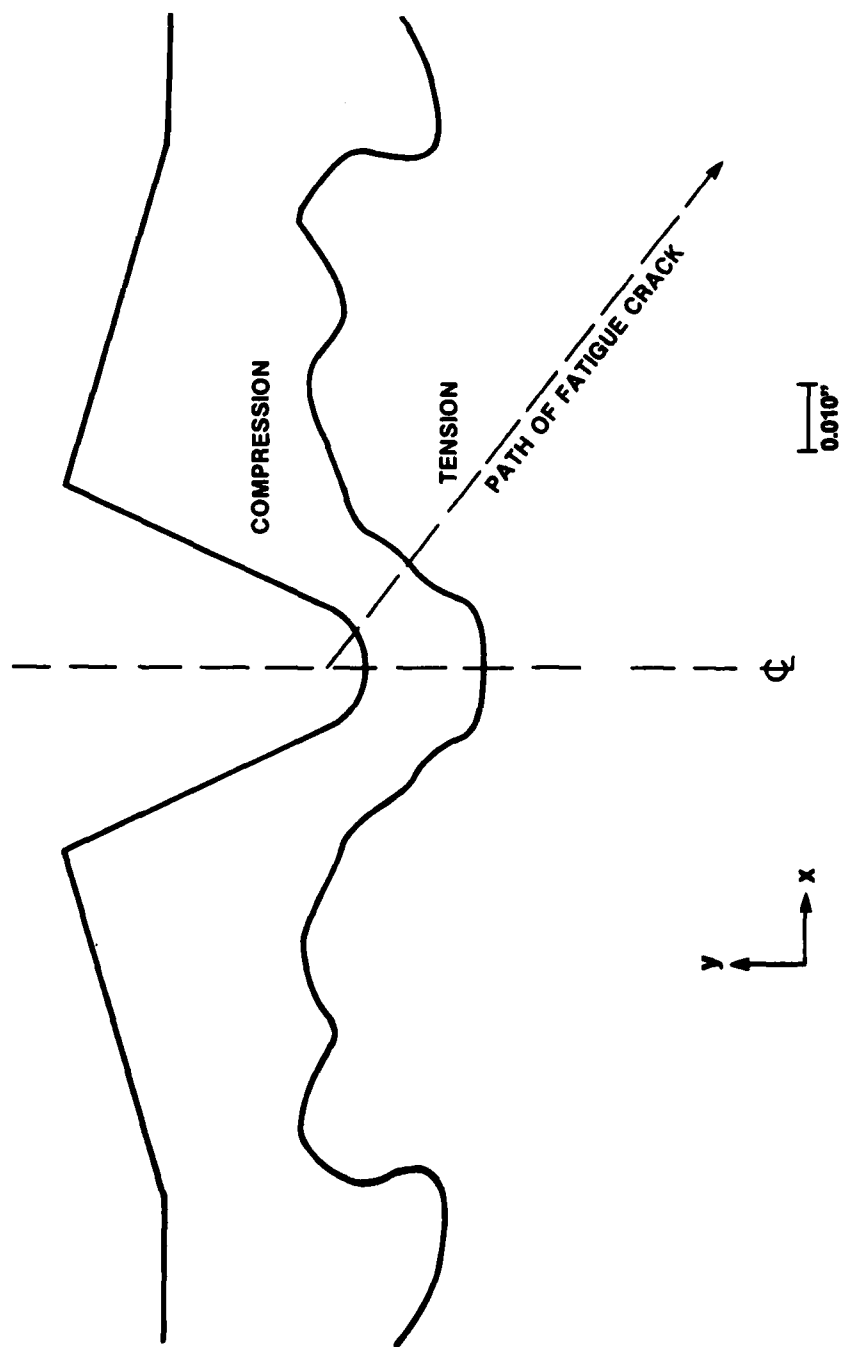


Figure 16 - Predicted Residual Stresses in the x Direction Resulting From Notch Rolling

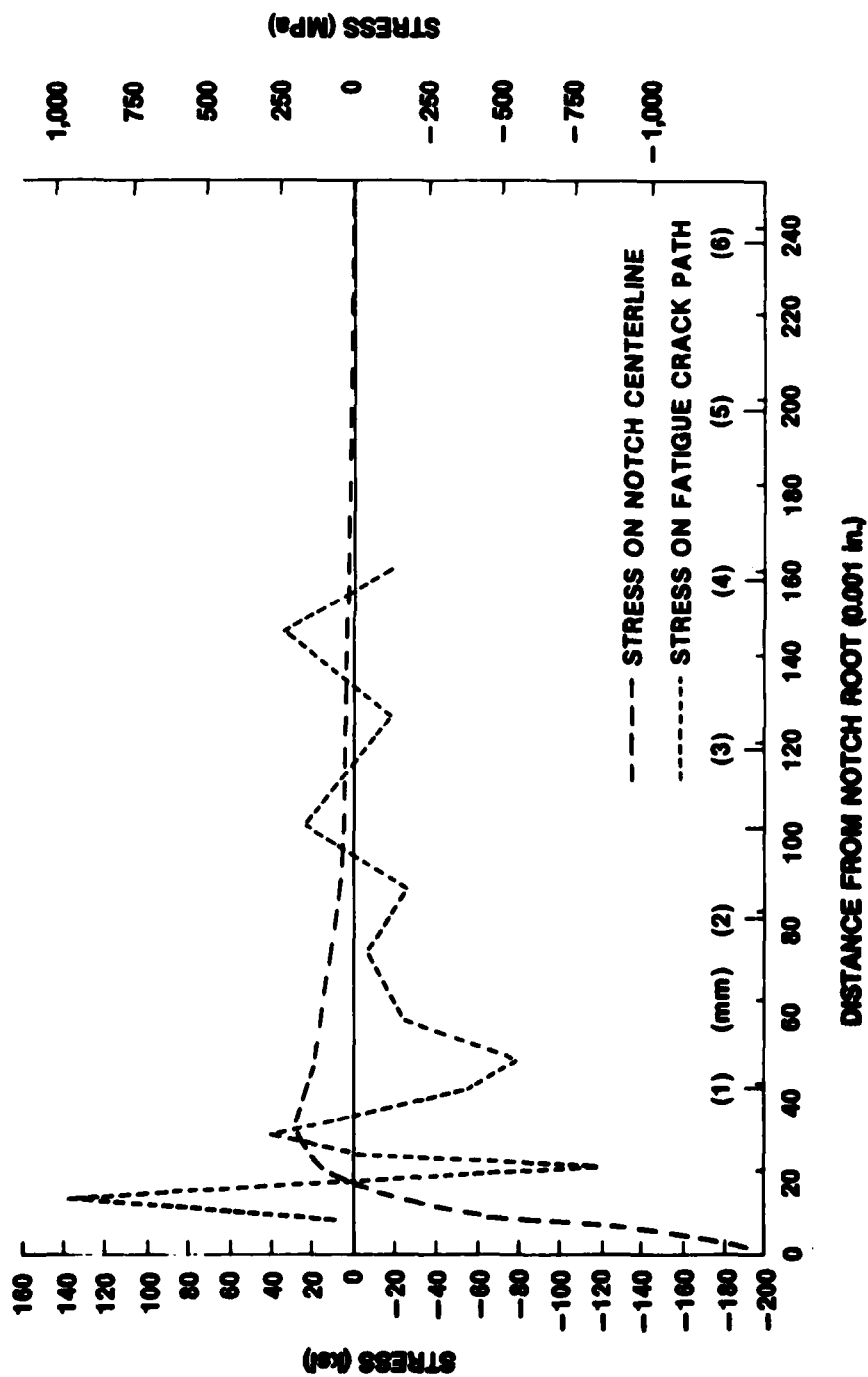


Figure 17 - Predicted Residual Stresses Resulting From Notch Rolling

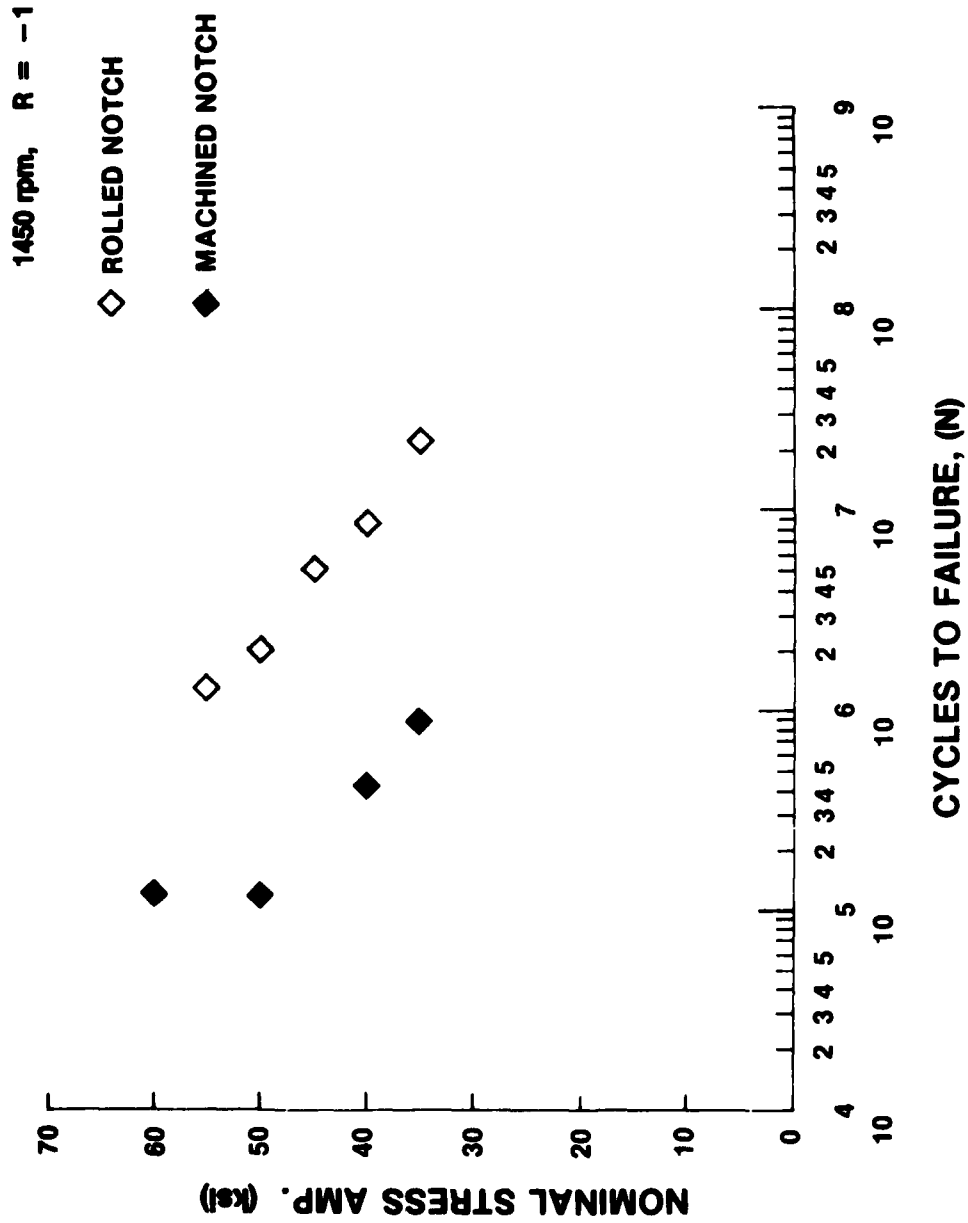


Figure 18 - Results of Rotating Cantilever-Beam Fatigue Tests of Inconel 718
With Machined and Rolled Notches



Figure 19 - Fracture Surface of Machined and Rolled
Notch Fatigue Specimens

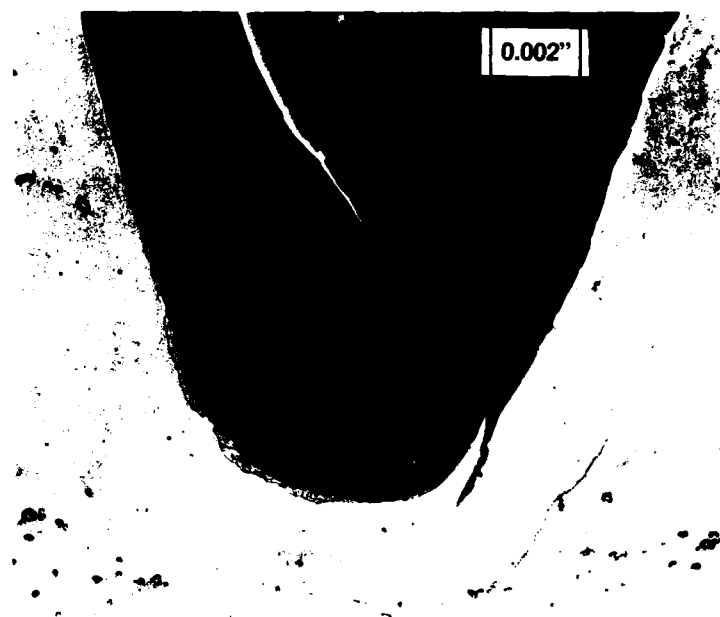


Figure 20 - Photomicrograph of Cross Section
of a Rolled Notch in a Round Specimen
(0.560-In. Diameter) of Inconel 718



Figure 21 - Photomicrograph of the Notch
Cross Section Showing the Notch Root
Fatigue Crack Which Caused Failure
(Upper Right) (50X)
(Etchant: $\text{HNO}_3 + \text{HF} + \text{H}_2\text{O}$
for 2-3 Minutes)

REFERENCES

1. Föppl, O., "Die Steigerung der Dauerhaltbarkeit durch Oberflächendrücken," *Maschinenbau*, Vol. 8 (1929), p. 752.
2. Hoger, O.J. and J.L. Maultbetsch, "Increasing the Fatigue Strength of Press-Fitted Axle Assemblies by Surface Rolling," *Transactions of the American Society of Mechanical Engineers*, Vol. 58 (1936), pp. A9-A98.
3. Frost, N.E., "Effect of Cold Work on the Fatigue Properties of Two Steels," *Metallurgia*, Vol. 59 (1960), pp. 85-90.
4. Field, J.E., "Fatigue Strength of Cold-Rolled Threads," *Engineer* (1968), pp. 974-976.
5. Bellow, D.G. and Faulkner, "Salt Water and Hydrogen Sulfide Corrosion Fatigue of Work Hardened Threaded Elements," *Journal of Testing and Evaluation*, Vol. 4 (Mar 1976), pp. 141-147.
6. Fuchs, H.O., "Prestressing and Fatigue," *Metals Engineering Quarterly* (Aug 1966), pp. 59-62.
7. "Fatigue An Interdisciplinary Approach," Sagamore Army Materials Research Conference (Syracuse, NY: Syracuse University Press, 1964), p. 45.
8. Froeh, et al., "Metal Fatigue," (Oxford, Gr. Britain: Clarendon Press, 1974), p. 404.
9. Grunzweig, J. et al., "Calculations and Measurements on Wedge Indentation," *Journal of the Mechanics and Physics of Solids*, Vol. 2 (1954), pp. 81-86.
10. Johnson, W. et al., "Further Experiments Concerning Geometrically Similar Indentations," *International Journal of Mechanics and Science*, Vol. 8 (1973), pp. 49-59.
11. Hill, R., "Mathematical Theory of Plasticity, The," (London, U.K.: Oxford University Press, 1950), p. 23.

12. Backofen, W.A., "Deformations Processing," (Reading, Mass.: Addison-Wesley Publishing Co., 1972), p. 23.

13. "Manual on Fatigue Testing," STP 91, (Philadelphia, PA: ASTM, 1949), p. 30.

14. Shatinskii, V.F., "Thermomechanical Surface Treatment as Applied to Steel 40Kh," Soviet Materials Science, Vol. 2, (Jan-Feb 1966), pp. 82-87.

INITIAL DISTRIBUTION

Copies

9 NAVSEA

1 SEA 05D
1 SEA 05R/Miller
1 SEA 05R15/Vanderveldt
1 PMS 389
1 PMS 399
1 SEA 521
1 SEA 524
2 SEA 99612

12 DTIC

CENTER DISTRIBUTION

Copies	Code	Name
1	1720.3	R. Jones
1	1720.6	R. Rockwell
1	2809H	J. Hudak
5	281	G. Wacker
10	2814	J. Gudas
5	2814	M. Vassilaros
1	282	J. Crisci
1	522.1	Unclass Library
2	5231	Office Services

DTNSRDC ISSUES THREE TYPES OF REPORTS

1. DTNSRDC REPORTS, A FORMAL SERIES, CONTAIN INFORMATION OF PERMANENT TECHNICAL VALUE. THEY CARRY A CONSECUTIVE NUMERICAL IDENTIFICATION REGARDLESS OF THEIR CLASSIFICATION OR THE ORIGINATING DEPARTMENT.

2. DEPARTMENTAL REPORTS, A SEMIFORMAL SERIES, CONTAIN INFORMATION OF A PRELIMINARY, TEMPORARY, OR PROPRIETARY NATURE OR OF LIMITED INTEREST OR SIGNIFICANCE. THEY CARRY A DEPARTMENTAL ALPHANUMERICAL IDENTIFICATION.

3. TECHNICAL MEMORANDA, AN INFORMAL SERIES, CONTAIN TECHNICAL DOCUMENTATION OF LIMITED USE AND INTEREST. THEY ARE PRIMARILY WORKING PAPERS INTENDED FOR INTERNAL USE. THEY CARRY AN IDENTIFYING NUMBER WHICH INDICATES THEIR TYPE AND THE NUMERICAL CODE OF THE ORIGINATING DEPARTMENT. ANY DISTRIBUTION OUTSIDE DTNSRDC MUST BE APPROVED BY THE HEAD OF THE ORIGINATING DEPARTMENT ON A CASE-BY-CASE BASIS.